

# Omeprazole Attenuates Pulmonary Aryl Hydrocarbon Receptor Activation and Potentiates Hyperoxia-Induced Developmental Lung Injury in Newborn Mice

Binoy Shivanna,<sup>1</sup> Shaojie Zhang, Ananddeep Patel, Weiwu Jiang, Lihua Wang, Stephen E. Welty, and Bhagavatula Moorthy

Section of Neonatal-Perinatal Medicine, Department of Pediatrics, Texas Children's Hospital, Baylor College of Medicine, Houston, Texas 77030

<sup>1</sup>To whom correspondence should be addressed at Division of Neonatal-Perinatal Medicine, Texas Children's Hospital, Baylor College of Medicine, 1102 Bates Avenue, MC: FC530.01, Houston, TX 77030. Fax: (832) 825 3204. E-mail: shivanna@bcm.edu

## ABSTRACT

Hyperoxia contributes to the development of bronchopulmonary dysplasia (BPD) in human preterm infants and a similar lung phenotype characterized by alveolar simplification in newborn mice. Omeprazole (OM) is a proton pump inhibitor that is used to treat humans with gastric acid related disorders. OM-mediated aryl hydrocarbon receptor (AhR) activation attenuates acute hyperoxic lung injury (HLI) in adult mice. Whether OM activates pulmonary AhR and protects C57BL/6J newborn mice against hyperoxia-induced developmental lung (alveolar and pulmonary vascular simplification, inflammation, and oxidative stress) injury (HDLI) is unknown. Therefore, we tested the hypothesis that OM will activate pulmonary AhR and mitigate HDLI in newborn mice. Newborn mice were treated daily with i.p. injections of OM at doses of 10 (OM10) or 25 (OM25) mg/kg while being exposed to air or hyperoxia (FiO<sub>2</sub> of 85%) for 14 days, following which their lungs were harvested to determine alveolarization, pulmonary vascularization, inflammation, oxidative stress, vascular injury, and AhR activation. To our surprise, hyperoxia-induced alveolar and pulmonary vascular simplification, inflammation, oxidative stress, and vascular injury were augmented in OM25-treated animals. These findings were associated with attenuated pulmonary vascular endothelial growth factor receptor 2 expression and decreased pulmonary AhR activation in the OM25 group. We conclude that contrary to our hypothesis, OM decreases functional activation of pulmonary AhR and potentiates HDLI in newborn mice. These observations are consistent with our previous findings, which suggest that AhR activation plays a protective role in HDLI in newborn mice.

**Key words:** omeprazole; aryl hydrocarbon receptor; hyperoxia; lung development; inflammation; oxidative stress

Bronchopulmonary dysplasia (BPD) is a chronic lung disease of infancy that is characterized by an interruption of lung alveolar and vascular growth (Husain *et al.*, 1998; Jobe, 1999). Despite improved therapies of premature infants, BPD remains the most prevalent, and one of the most serious long-term sequelae of preterm birth, affecting approximately 14 000 preterm infants born each year in the United States (Fanaroff *et al.*, 2007). Furthermore, infants with BPD are more likely to have long-

term pulmonary problems, increased rehospitalizations during the first year of life, and delayed neurodevelopment (Fanaroff *et al.*, 2007; Short *et al.*, 2003). Hence, there is an urgent need for improved therapies to prevent and treat BPD. Evidence implicates hyperoxia-induced reactive oxygen species generation and lung inflammation as major contributors in the development of BPD (Saugstad, 2003). Hyperoxia-induced lung injury in neonatal mice leads to a phenotype (Park *et al.*, 2007), which is

similar to human BPD. We utilized this model to delineate the role of aryl hydrocarbon receptor (AhR) signaling in neonatal hyperoxia-induced lung injury.

The AhR is a member of basic—helix—loop—helix/PER—ARNT—SIM family of transcriptional regulators (Sogawa and Fujii-Kuriyama, 1997). The AhR is expressed in all mouse tissues (Abbott et al., 1995), and in humans, AhR is highly expressed in the lungs, thymus, kidney, and liver (Tirona and Kim, 2005). The AhR is predominantly cytosolic, localized in a core complex comprising 2 molecules of 90-kDa heat shock protein and a single molecule of the cochaperone hepatitis X-associated protein-2 (Carver and Bradfield, 1997; Denis et al., 1988). Ligand binding to the AhR results in a conformational change of the cytosolic AhR complex that exposes the nuclear localization sequence(s), resulting in translocation of this complex into the nucleus (Pollenz et al., 1994). In the nucleus, AhR dissociates from the core complex, dimerizes with the AhR nuclear translocator, and initiates transcription of many phase I and phase II antioxidant enzymes (AOE) such as cytochrome P450 (CYP) 1A1 and NAD(P)H quinone reductase-1 (NQO1), by its interaction with the xenobiotic responsive elements present in the promoter region of these genes (Favreau and Pickett, 1991; Fujisawa-Sehara et al., 1987). Recently, we observed that newborn AhR dysfunctional (AhRd) mice (Shivanna et al., 2013) and AhR-deficient primary fetal human pulmonary microvascular endothelial cells (Zhang et al., 2015) have an increased susceptibility to hyperoxic lung injury (HLI) that is associated with decreases in the expression of phase I (CYP 1A) and phase II (NQO1) AOE and increased inflammation, suggesting that AhR activation mediates processes suppressing lung oxidative stress and inflammation. Hence, this study was aimed to address the knowledge gap of whether pharmacological AhR activation is sufficient to protect the newborn mice against HLI.

Omeprazole (OM), a substituted benzimidazole derivative, is a proton pump inhibitor that inhibits gastric acid secretion both in humans (Lind et al., 1983) and in animals (Larsson et al., 1983). It has been widely used in the management of gastric acid related disorders in humans for decades (Li et al., 2004). Studies have shown that OM activates AhR in human and rat hepatocytes (Diaz et al., 1990; Kashfi et al., 1995). Additionally, we observed that OM attenuated hyperoxic injury in adult mice *in vivo* (Shivanna et al., 2011b) and in adult human H441 cells *in vitro* (Shivanna et al., 2011a) via activation of the AhR, which was associated with decreased hyperoxia-induced oxidative stress and inflammation. Whether OM activates pulmonary AhR and protects C57BL/6J newborn mice against hyperoxia-induced developmental lung (alveolar and pulmonary vascular simplification, inflammation, and oxidative stress) injury (HDLI) is unknown. Therefore, in this study we tested the hypothesis that OM will activate pulmonary AhR and mitigate HDLI in C57BL/6J newborn mice.

## MATERIALS AND METHODS

### Animals

This study was approved and conducted in strict accordance with the federal guidelines for the humane care and use of laboratory animals by the Institutional Animal Care and Use Committee of Baylor College of Medicine (Protocol number: AN-5631). The C57BL/6J mice were obtained from The Jackson Laboratory (Bar Harbor, Maine). Time pregnant mice raised in our animal facility were used for the experiments.

### OM Dose Response Studies

One-day old C57BL/6J newborn mice were injected intraperitoneally with either 10, 25, or 50 mg/kg of OM or the vehicle, polyethylene glycol (PEG) (Tallman et al., 2004), once daily for 4 days ( $n=4$  per group). These animals were maintained in room air conditions and not exposed to hyperoxia. At the end of the experiments, the animals were anesthetized with 200 mg/kg of *i.p.* sodium pentobarbital and killed by exsanguination while under deep pentobarbital anesthesia. The lung tissues were harvested only for analysis of CYP1A1 induction.

### Treatment and Exposure

Within 24 h of birth, pups from multiple litters were pooled before being randomly and equally redistributed to the dams, following which they were injected daily with *i.p.* injections of the vehicle, PEG (Tallman et al., 2004), or with OM at a dose of 10 (OM10) or 25 (OM25) mg/kg while being exposed to either 21% O<sub>2</sub> (air) or 85% O<sub>2</sub> (hyperoxia) for 14 days. The dams were rotated between air- and hyperoxia-exposed litters every 48 h to prevent oxygen toxicity in the dams and to eliminate maternal effects between the groups. Oxygen exposures were conducted in Plexiglas chambers and the animals were monitored as described previously (Shivanna et al., 2013).

### Tissue Preparation for Lung Morphometry, Immunohistochemistry, and Analyses of Vascularization, Oxidative Stress, and AhR Activation

After completion of experiments, a subset of pups were killed and their lungs were inflated and fixed via the trachea with 10% formalin at 25 cm H<sub>2</sub>O pressure for at least 10 min and sections of the paraffin embedded lungs were obtained for the analysis of lung morphometry as described previously (Shivanna et al., 2013). The right and left lungs ( $n=6$  per group) from a separate group of study animals were snap frozen in liquid nitrogen and stored at  $-80^{\circ}\text{C}$  for subsequent isolation of total proteins and RNA, respectively.

### Analyses of Alveolarization

**Lung morphometry.** Alveolar development on selected mice ( $n=6$  per group) was evaluated by radial alveolar counts (RAC) and mean linear intercepts (MLI). The observers performing the measurements were masked to the slide identity. (1) Radial alveolar counts: RAC was determined as described by Cooney and Thurlbeck (1982). RAC measurements were made by dropping a perpendicular line from the center of a respiratory bronchiole to the edge of the septum or pleura and counting the number of alveoli traversed by this line. (2) Mean linear intercepts: MLIs were assessed as described previously (van Eijl et al., 2011). Briefly, grids of horizontal and vertical lines were superimposed on an image and the number of times the lines intersected with the tissue was counted. The total length of the grid lines was then divided by the number of intersections, to provide the MLI in  $\mu\text{m}$ . Photographs from at least 10 random non-overlapping lung fields (10 $\times$  magnification) were taken from each animal for RAC and MLI measurements.

**Analyses of pulmonary vascularization.** Pulmonary vessel density was determined based on immunohistochemical staining for von Willebrand factor (vWF), which is an endothelial specific marker. At least 10 counts from 10 random non overlapping fields (20 $\times$  magnification) was performed for each animal ( $n=6$  per group). The observers performing the measurements were masked to the slide identity.

**Analyses of lung inflammation.** Lung inflammation was assessed by immunostaining for macrophages: Deparaffinized lung sections were stained with rat antimouse Mac-3 antibody (BD Pharmingen; 553322, dilution 1:750), followed by staining with the appropriate biotinylated secondary antibody (Vector Laboratories, Burlingame, California). Although Mac-3 can be expressed on other myeloid cells such as monocytes, we used this marker to quantify the cells in the lung tissue rather than in the lung blood vessels and therefore the stained cells are most likely to be macrophages. The number of macrophages in the alveolar and interstitial spaces was counted from at least 10 random nonoverlapping lung fields (40× magnification) per animal ( $n = 6$  per group). The observers performing the macrophage counts were masked to the slide identity.

**Bronchoalveolar lavage.** BAL was performed in selected mice ( $n = 6$  per group) after completion of experiments as described previously. BAL fluid (BALF) supernatant was used to analyze the protein concentration by Bradford method (Bradford, 1976).

**Analysis of lung oxidative stress.** Malondialdehyde (MDA) is a stable end product of lipid peroxidation and is a generally accepted marker of oxidative stress (Del Rio et al., 2005). Likewise, nitrotyrosine (NT) is a product of tyrosine nitration that results from a combination of oxidative and nitrative stress (Ischiropoulos, 1998). Hence, we performed western blotting on lung proteins using anti-MDA (Cell Biolabs, Inc, San Diego, California; STA-331, dilution 1:1000), anti-NT (Cell Biolabs; STA-303, dilution 1:1000), and anti- $\beta$ -actin (Santa Cruz Biotechnologies, Santa Cruz, California; sc-47778, dilution 1:2000) antibodies as per the manufacturer's recommendations to assess oxidative stress.

**Analyses of the pulmonary AhR activation.** It is reported that functional activation of the AhR results in the expression of several phases I and II enzymes. So, we determined the functional activation of the pulmonary AhR by determining the expression of pulmonary CYP1A1 (phase I), and NQO1 (phase II) enzymes. Additionally, we determined pulmonary AhR expression at the mRNA and protein levels.

**Quantitative real-time RT-PCR assays.** Total RNA extracted from frozen lung tissues using Direct-zol RNA MiniPrep kit (Zymo Research, Irvine, California; R2052) as per the manufacturer's recommendations and reverse transcribed to cDNA as described before (Zhang et al., 2015). Real-time quantitative RT-PCR analysis was performed with 7900HT Real-Time PCR System using TaqMan gene expression master mix (Grand Island, New York; 4369016) and gene specific primers (Grand Island, New York; AhR-Mm00478932\_m1; CYP1A1-Mm00487218\_m1; GAPDH-Mm99999915\_g1; NQO1-Mm01253561\_m1; VEGF-Mm01281449\_m1; and VEGFR2- Mm01222421-m1). GAPDH was used as the reference gene. The samples were denatured at 95°C for 10 min followed by a thermal cycling step of 40 cycles at 95°C for 15 s and 40 cycles at 60°C for 1 min. The  $\Delta\Delta C_t$  method was used to calculate the fold change in mRNA expression (Jiang et al., 2004).

#### Western Blot Assays

The protein extracts from the experimental animals were separated by 10% SDS-polyacrylamide gel electrophoresis and transferred to polyvinylidene difluoride membranes. The membranes were incubated overnight at 4°C with the following primary antibodies: anti-AhR (Enzo Life Sciences, Farmingdale, New York; BML-SA210-0100, dilution 1:2000), anti- $\beta$ -actin (Santa

Cruz Biotechnologies; sc-47778, dilution 1:2000), anti-CYP1A1 (gift from P.E. Thomas, Rutgers University, Piscataway, New Jersey, dilution 1:1500), anti-NQO1 (Santa Cruz Biotechnologies; sc-16464, dilution 1:500), anti-vascular endothelial growth factor receptor A (VEGF-A) (Santa Cruz Biotechnologies; sc-152, dilution 1:500), and anti-VEGF receptor 2 (VEGFR2) (Cell Signaling, Danvers, Massachusetts; 2479, dilution 1:1000) antibodies. The primary antibodies were detected by incubation with the appropriate horseradish peroxidase-conjugated secondary antibodies. The immunoreactive bands were detected by chemiluminescence methods and the band density was analyzed by Image J software (National Institutes of Health, Bethesda, Maryland).

#### Statistical Analyses

The results were analyzed by GraphPad Prism 5 software. Data are expressed as means  $\pm$  SEM. The effects of the medication (OM), exposure, and their associated interactions for the outcome variables were assessed using ANOVA techniques. Multiple comparison testing by the post hoc Bonferroni test was performed if statistical significance of either variable or interaction was noted by ANOVA. A  $p < .05$  was considered significant.

## RESULTS

In this study, we investigated the role of OM on pulmonary AhR signaling and HDLI in newborn WT mice.

#### Short Term (4 Days) OM Therapy Activates Pulmonary AhR in a Dose-Dependent Manner in Newborn Mice

To determine whether OM activates pulmonary AhR, we treated newborn mice with incremental doses of OM (10–50 mg/kg/d i.p.) for 4 days, following which we examined the expression of the AhR-regulated pulmonary CYP1A1 enzyme. Omeprazole increased pulmonary CYP1A1 mRNA (Fig. 1A) and protein (Figs. 1B and 1C) expression in a dose-dependent manner with the minimum effective dose being 25 mg/kg/day.

#### OM Increases Hyperoxia-Induced Alveolar Simplification in a Dose-Dependent Manner

We investigated the effects of OM on hyperoxia-induced alveolar simplification by exposing the OM-treated animals to hyperoxia. Alveolar simplification was determined by RAC and MLI. Exposure of mice to 14 days of hyperoxia resulted in a significant decrease in RAC (Figs. 2A–F and 2G) indicating that their alveoli were fewer in number compared to corresponding air-breathing animals. In addition, hyperoxia-exposed mice had significant increases in MLI (Figs. 2A–F and 2H) indicating that their alveoli were also larger than in the corresponding air-breathing animals. Surprisingly, hyperoxia-induced alveolar simplification was significantly increased in OM25-treated animals than in those exposed to the vehicle, PEG, only or OM10-treated mice (Figs. 2A–H). Statistical analyses indicated a significant 2-way interaction between hyperoxia and OM25 treatment on alveolarization. In air-breathing animals, there was no significant difference in alveolarization between PEG (Figs. 2A, 2G, and 2H) and OM10 (Figs. 2B, 2G, and 2H) or OM25 (Figs. 2C, 2G, and 2H) treated mice.

#### OM Increases Hyperoxia-Induced Pulmonary Vascular Simplification in a Dose-Dependent Manner

We next examined the effects of OM on hyperoxia-induced pulmonary vascular simplification by quantifying the vWF stained lung blood vessels in the animals exposed to hyperoxia.

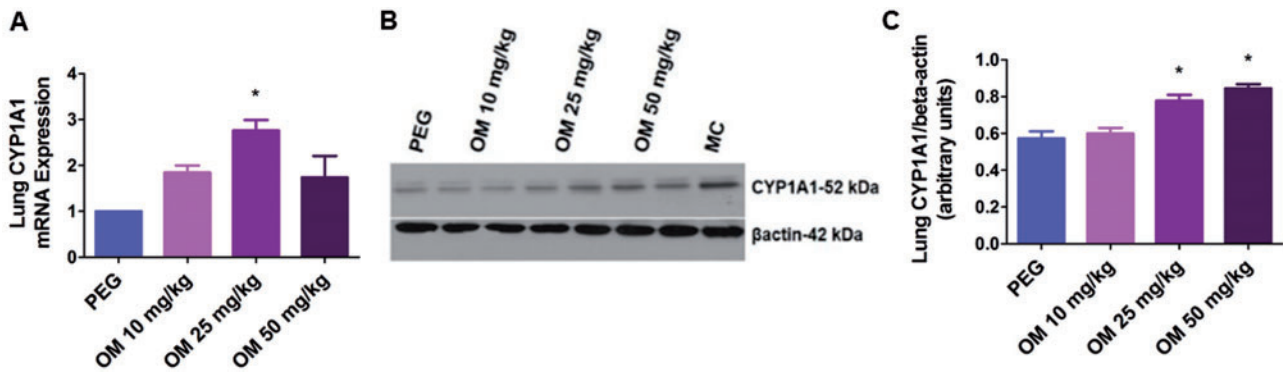


FIG. 1. OM increases pulmonary CYP1A1 mRNA and protein expression in newborn mice: Newborn mice were treated with the vehicle, polyethylene glycol (PEG), or with 10, 25, or 50 mg/kg of OM i.p. once daily for 4 days, following which lung CYP1A1 mRNA (A) and protein (B) expression were determined by real-time RT-PCR analysis and western blotting, respectively. CYP1A1 band intensities were quantified and normalized to  $\beta$ -actin (C). Values are means  $\pm$  SEM from at least 4 individual animals per group. Significant differences between PEG and OM groups are indicated by \* $p < .05$ .

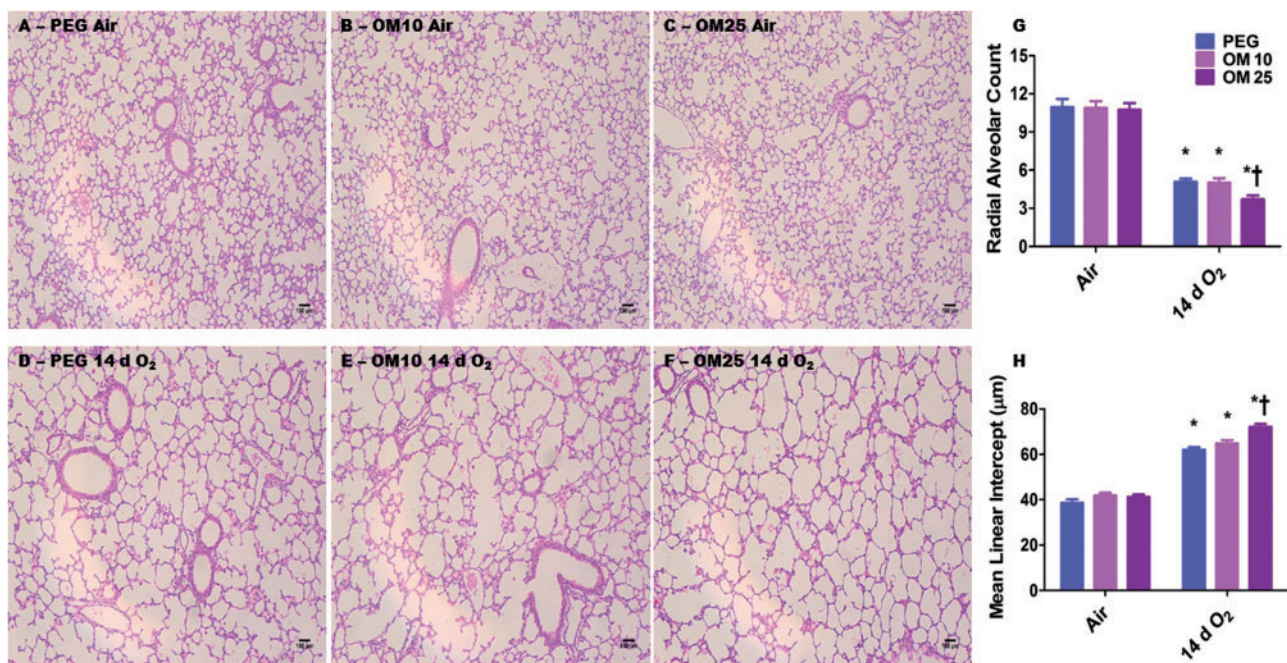


FIG. 2. OM25-treated mice have increased hyperoxia-induced alveolar simplification. A-F, Representative hematoxylin and eosin-stained lung sections obtained from PEG (A and D), OM10 (B and E), or OM25 (C and F) treated newborn mice exposed to air (A-C) or hyperoxia (D-F) for 14 days. Alveolarization was quantified by radial alveolar count (G) and MLIs (H). Values are means  $\pm$  SEM from at least 6 individual animals per group. Two-way ANOVA showed an effect of hyperoxia and OM25 treatment and an interaction between them for the dependent variables, RAC and MLI. Significant differences between air-breathing and hyperoxia-exposed animals are indicated by \* $p < .05$ . Significant differences between vehicle and OM-treated mice exposed to hyperoxia are indicated by † $p < .05$ . Scale bar = 100  $\mu$ m.

Exposure to hyperoxia resulted in pulmonary vascular simplification as evidenced by decreased vWF stained lung blood vessels (Figs. 3D-G). Consistent with its effects on alveolar simplification, OM25 augmented hyperoxia-induced pulmonary vascular simplification (Figs. 3D-G). In air-breathing animals, there was no significant difference in pulmonary vascularization between PEG (Figs. 3A and 3G) and OM10 (Figs. 3B and 3G) or OM25 (Figs. 3C and 3G) treated mice.

#### OM Augments Hyperoxia-Induced Decrease in Lung VEGFR2 Protein Expression

Having observed the effects of OM on pulmonary vascular simplification, we determined the expression of VEGFR2 and VEGF since they play a crucial role in pulmonary vascular development. Hyperoxia decreased the expression of both VEGFR2 and

VEGF at the mRNA (Figs. 4A and 4D) and protein levels (Figs. 4B, 4C, 4E, and 4F). Interestingly, OM augmented hyperoxia-induced decrease in VEGFR2 protein expression (Figs. 4B and 4C). However, VEGFR2 mRNA (Fig. 4A) and VEGF mRNA (Fig. 4D) and protein (Figs. 4E and 4F) expression were similar in the vehicle- and OM-treated animals both in air and hyperoxic conditions.

#### OM Increases Hyperoxia-Induced Lung Macrophage Influx and Vascular Injury in a Dose-Dependent Manner

We performed immunohistochemical studies on fixed lung sections using anti-Mac-3 antibodies to ascertain if OM altered hyperoxia-induced lung macrophage accumulation. The immunohistochemistry studies revealed that hyperoxia increased accumulation of lung macrophages (Figs. 5D-G) in the animals. However, the effects of hyperoxia-induced lung macrophage

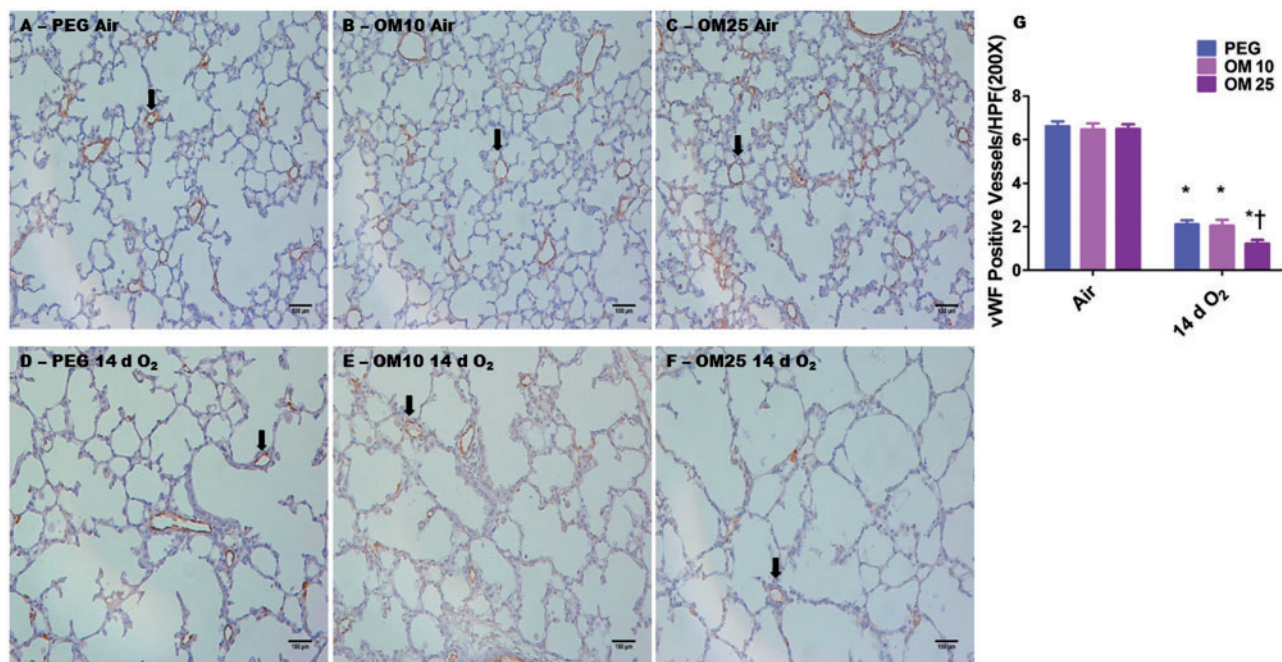


FIG. 3. OM25 augments hyperoxia-induced decrease in pulmonary blood vessel density. A-F, Representative vWF stained lung blood vessels obtained from PEG (A and D), OM10 (B and E), or OM25 (C and F) treated newborn mice exposed to air (A-C) or hyperoxia (D-F) for 14 days. G, Quantitative analysis of vWF stained lung blood vessels per high power field. Values are means  $\pm$  S.E.M. from at least 6 individual animals per group. Two-way ANOVA showed an effect of hyperoxia and OM25 treatment and an interaction between them for the dependent variable, vWF stained lung blood vessels. Significant differences between air-breathing and hyperoxia-exposed animals are indicated by \* $p < 0.05$ . Significant differences between vehicle and OM-treated mice exposed to hyperoxia are indicated by † $p < 0.05$ . Arrows point to brown staining lung blood vessels. Scale bar = 100  $\mu$ M.

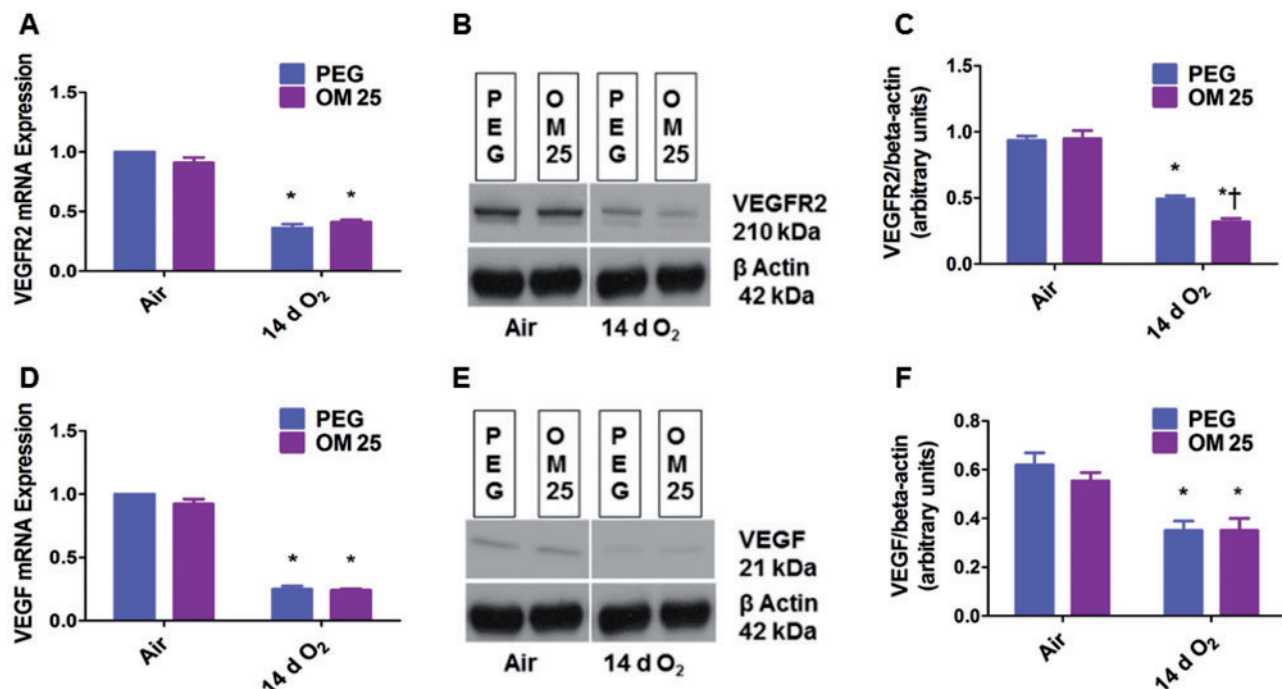


Fig. 4. OM25 augments hyperoxia-induced decrease in VEGFR2 protein expression. Newborn mice were treated with PEG or OM25 and exposed to air or hyperoxia for 14 days, following which pulmonary VEGFR2 mRNA (A) and protein (B) and VEGF mRNA (D) and protein (E) expression were determined by real-time RT-PCR analysis and western blotting. Densitometric analyses wherein VEGFR2 (C) and VEGF (F) band intensities were quantified and normalized to  $\beta$ -actin. Values are means  $\pm$  SEM from at least 6 individual animals per group. Two-way ANOVA showed an effect of hyperoxia on both VEGFR2 and VEGF, and an effect of OM25 treatment and an interaction between OM25 treatment and hyperoxia for the dependent variable, VEGFR2 protein level. Significant differences between air-breathing and hyperoxia-exposed animals are indicated by \* $p < 0.05$ . Significant differences between vehicle and OM-treated mice exposed to hyperoxia are indicated by † $p < .05$ .

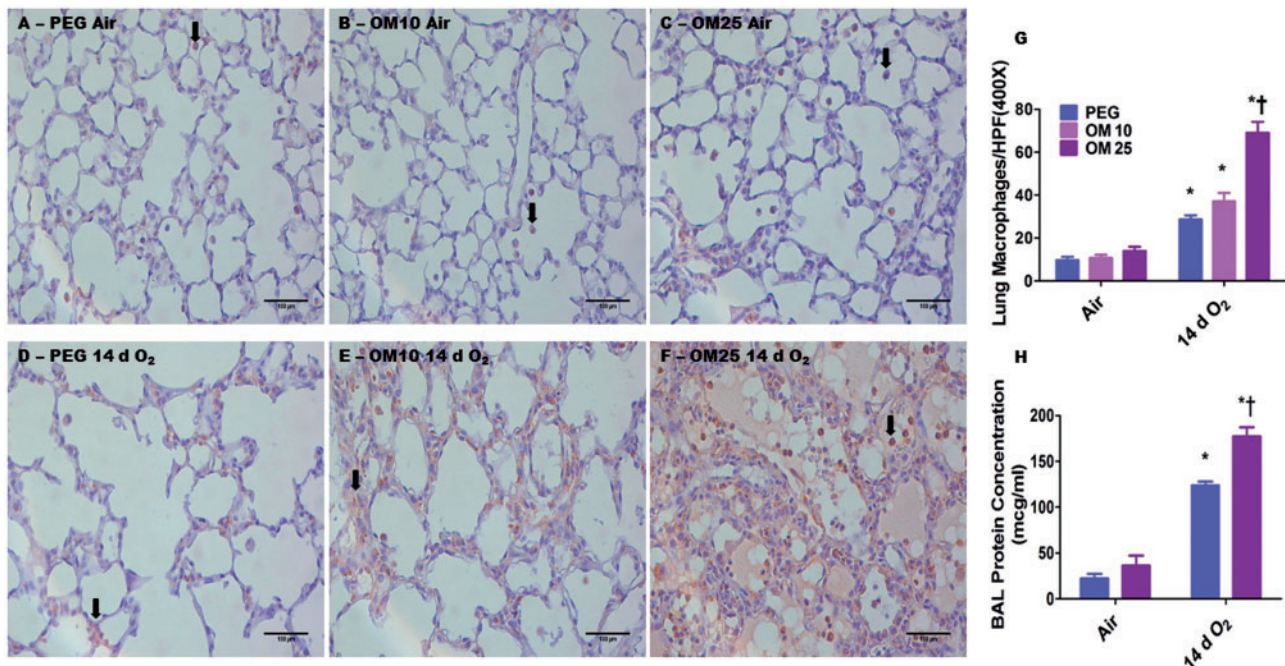


FIG. 5. OM25-treated newborn mice have increased hyperoxia-induced lung inflammation and vascular injury. A–F, Representative Mac 3 antibody immunostained lung sections obtained from PEG (A and D), OM10 (B and E), or OM25 (C and F) treated newborn mice exposed to air (A–C) or hyperoxia (D–F) for 14 days. G, Quantitative analysis of macrophages per high power field. H, Quantitative analysis of bronchoalveolar lavage fluid (BALF) protein levels. Values are means  $\pm$  SEM from at least 6 individual animals per group. Two-way ANOVA showed an effect of hyperoxia and OM25 treatment and an interaction between them for the dependent variables, lung macrophages and BALF protein levels. Significant differences between air-breathing and hyperoxia-exposed animals are indicated by \* $p < 0.05$ . Significant differences between vehicle and OM-treated mice exposed to hyperoxia are indicated by † $p < 0.05$ . Arrows point to brown staining lung macrophages. Scale bar = 100  $\mu$ m.

influx was augmented in mice treated with OM 25 (Figs. 5F and 5G) compared to mice treated with PEG (Figs. 5D and 5G) or OM10 (Figs. 5E and 5G). Additionally, we estimated BALF protein levels to determine the effects of OM on the pulmonary vasculature. Consistent with its adverse effects on lung alveolarization and inflammation, OM25 therapy increased hyperoxia-induced BALF protein levels (Fig. 5H), which suggests that OM25 therapy increases lung vascular injury compared to vehicle-treated animals. Statistical analyses indicated a significant 2-way interaction between the between hyperoxia and OM25 treatment on lung inflammation and vascular injury. In air-breathing animals, there was no significant difference in lung macrophage counts between PEG (Figs. 5A and 5G) and OM10 (Figs. 5B and 5G) or OM25 (Figs. 5C and 5G) treated mice. Additionally, there was no significant difference in BALF protein levels between PEG and OM25-treated mice (Fig. 5H) exposed to air.

#### OM Augments Hyperoxia-Induced Lung MDA Protein Adduct and NT Expression

Hyperoxia-induced oxidative stress is well known to contribute to hyperoxia-induced alveolar and pulmonary vascular simplification. So, we performed western blotting using anti-MDA and anti-NT antibodies to determine the effects of OM on hyperoxia-induced lung oxidative stress. Interestingly, hyperoxia increased lung MDA protein adduct (Figs. 6A and 6B) and NT (Figs. 6C and 6D) expression in the regions between 40 and 80 and 55–72 kDa, respectively. Similar to its effect on hyperoxia-induced lung inflammatory response, OM augmented hyperoxia-induced increase in lung MDA protein adduct (Figs. 6A and 6B) and NT (Figs. 6C and 6D) expression in the regions specified when compared to similarly exposed vehicle-treated animals.

#### Prolonged (2 Weeks) OM Therapy Decreases Pulmonary CYP1A1 mRNA and Protein Expression

Because our results of the effect of OM on HDLI were contrary to our working hypothesis, we next determined the effects of prolonged (2 weeks) OM therapy on pulmonary AhR activation. Functional activation of AhR results in transcriptional activation of phase I (CYP1A1) and II (NQO1) enzymes. Hence, we examined the expression of CYP1A1 and NQO1 mRNA and protein. Hyperoxia had differential effects on CYP1A1 mRNA and protein levels, with the former being decreased (Fig. 7A) and the latter being increased (Fig. 7B and 7C) when compared with air-exposed animals. Surprisingly, OM25 for 2 weeks decreased CYP1A1 mRNA (Fig. 7A) and protein (Fig. 7B and 7C) levels when compared with vehicle-treated mice both in air and hyperoxic conditions.

#### Prolonged (2 weeks) OM Therapy Decreases Hyperoxia-Induced Pulmonary NQO1 mRNA and Protein Expression

Next we looked at the effects of OM and hyperoxia on the AhR-regulated phase II enzyme, NQO1. Hyperoxia increased NQO1 mRNA (Fig. 8A) and protein levels (Fig. 8B and 8C). However, OM25 attenuated hyperoxia-induced increase in NQO1 mRNA (Fig. 8A) and protein (Fig. 8B and 8C) expression. In air-breathing animals there was no significant difference in lung NQO1 expression (Fig. 8) between the vehicle- and OM-treated mice.

#### Prolonged (2 Weeks) OM Therapy Does Not Affect Pulmonary AhR mRNA and Protein Expression

Since OM transcriptionally decreased the expression of CYP1A1 and NQO1 enzymes, we finally determined the effects of OM and hyperoxia on AhR mRNA and protein expression in our experimental model. Interestingly, hyperoxia decreased lung

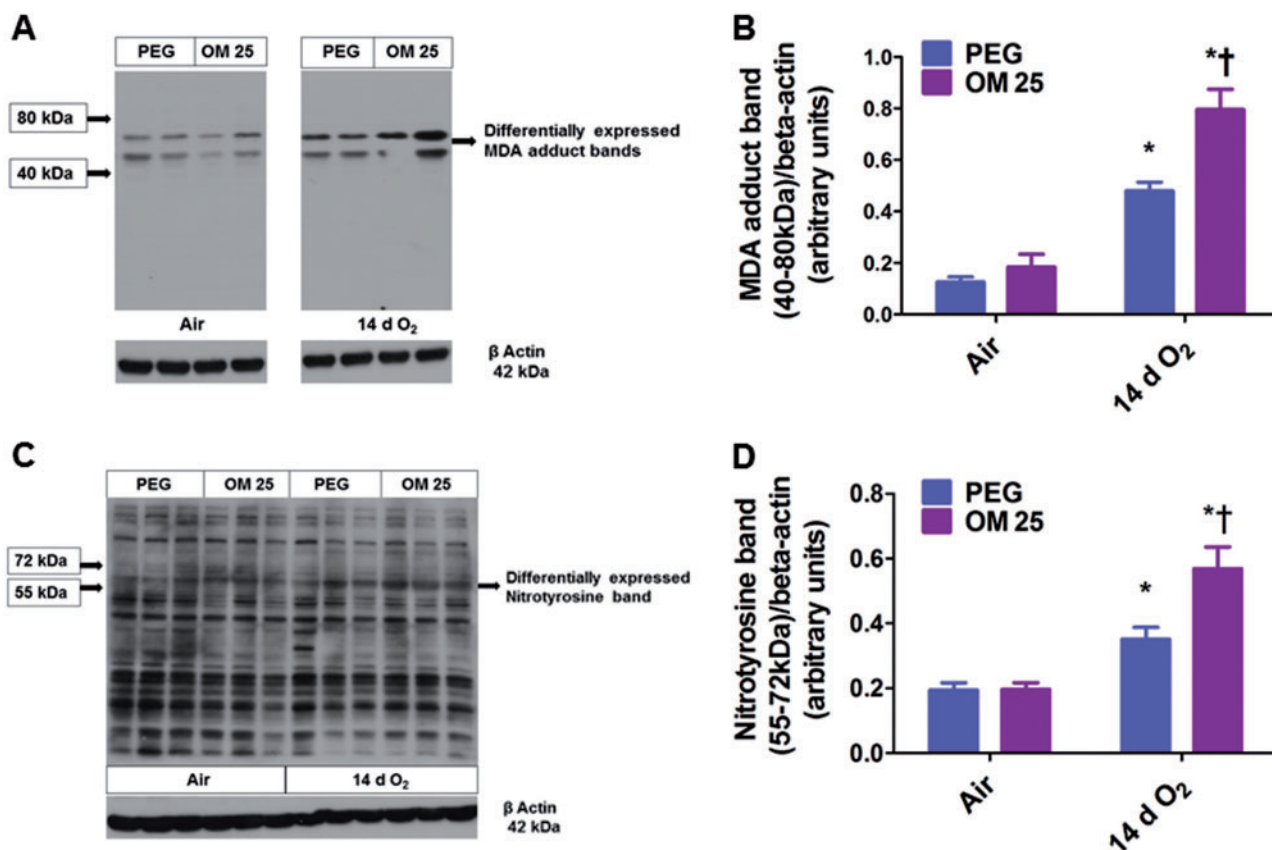


FIG. 6. OM25 augments hyperoxia-induced increase in lung MDA and NT levels. Lung protein obtained from newborn mice treated with PEG or OM25 and exposed to air or hyperoxia for 14 days was subjected to immunoblotting using anti-MDA, anti-NT, or  $\beta$ -actin antibodies. Representative western blots showing differential MDA protein adduct (A) and NT (C) expression in the regions between 40–80 kDa and 55–72 kDa, respectively. Densitometric analyses wherein the above MDA protein adduct (B) and NT (D) band intensities were quantified and normalized to  $\beta$ -actin. Values are means  $\pm$  S.E.M. from at least 6 individual animals per group. Two-way ANOVA showed an effect of hyperoxia and OM25 treatment and an interaction between them for the dependent variables, MDA protein adducts and NT in the above specified regions. Significant differences between air-breathing and hyperoxia-exposed animals are indicated by \*  $p < .05$ . Significant differences between vehicle and OM-treated mice exposed to hyperoxia are indicated by †  $p < .05$ .

AhR mRNA (Fig. 9A) and protein (Fig. 9B and 9C) levels. However, there was no significant difference in the lung AhR expression between the vehicle and OM25-treated animals both in air and hyperoxic conditions (Fig. 9).

## DISCUSSION

The present study demonstrates that prolonged (2 weeks) OM25 treatment potentiates HDLI in newborn WT mice via mechanisms entailing disruption of AhR signaling. In newborn mice *in vivo*, OM25-mediated increase in HLI correlated with attenuated expression of AhR-regulated phase I and II AOE and VEGFR2.

AhR is shown to be a crucial regulator of oxidant stress and inflammation through the induction of several detoxifying enzymes or via “cross-talk” with other signal transduction pathways (Baglolle *et al.*, 2008; Thatcher *et al.*, 2007). Whether increased pulmonary AhR signaling modulates neonatal HLI is unknown. To address this knowledge gap, we conducted experiments *in vivo* to activate pulmonary AhR and determine its role in HLI in newborn mice.

We initially studied the interaction between OM and pulmonary AhR. AhR activation results in the transcriptional induction of AhR gene battery, of which the best studied is CYP1A1 gene (Whitlock, 1999). Expectedly, OM induces AhR-dependent

CYP1A1 mRNA (Fig. 1A) and apoprotein (Fig. 1B and 1C) expression in newborn mice in a dose-dependent manner in short-term exposures (4 days). Although, Wei *et al.* (2002) observed that OM induces pulmonary CYP1A1 in adult human lung samples using an explant culture system, to the best of our knowledge, this is the first study to investigate the effects of OM on AhR signaling in newborn mice *in vivo*. We chose OM25 for our experiments because it was the minimum dose that activated pulmonary AhR in the short term exposure. Additionally, we used OM10 to determine the AhR independent effects of OM on hyperoxia-induced alveolar and pulmonary vascular simplification. We did not observe any toxic effects of OM in air breathing animals. The dose of OM used in this study was comparable to the dose used in previous studies (Kashfi *et al.*, 1995; Larsson *et al.*, 1988). Rodents require a considerably higher dose of OM than humans to induce CYP1A. Differential mechanisms by which OM enhance CYP1A gene transcription may be responsible for the differences observed among species (Tompkins and Wallace, 2007).

We next studied the effects of OM on hyperoxia-induced alveolar and pulmonary vascular simplification. Hyperoxia is known to cause alveolar and pulmonary vascular simplification both in preterm infants (Husain *et al.*, 1998; Jobe, 1999) and newborn mice (Park *et al.*, 2007). We observed similar findings (Figs. 2 and 3). However, the increase in hyperoxia-induced

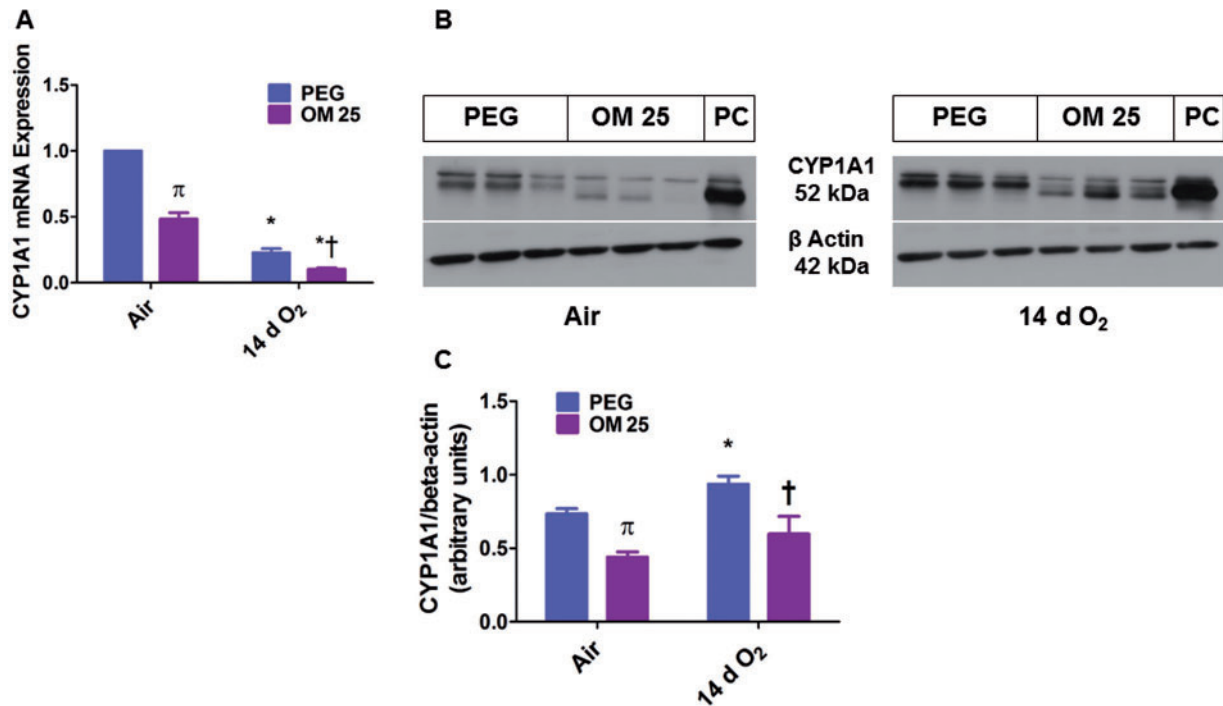


FIG. 7. Two weeks of OM25 therapy in newborn mice decreases pulmonary CYP1A1 mRNA and protein expression. Newborn mice were treated with PEG or OM25 and exposed to air or hyperoxia for 14 days, following which lung CYP1A1 mRNA (A) and protein (B) expression were determined by real-time RT-PCR analysis and western blotting, respectively. CYP1A1 band intensities were quantified and normalized to  $\beta$ -actin (C). Values are means  $\pm$  SEM from at least 6 individual animals per group. Two-way ANOVA showed an effect of exposure and OM25 treatment and an interaction between them for the dependent variable, CYP1A1. Significant differences between vehicle and OM-treated mice exposed to air are indicated by  $\pi$ ,  $p < .05$ . Significant differences between air-breathing and hyperoxia-exposed animals are indicated by \* $p < .05$ . Significant differences between vehicle and OM-treated mice exposed to hyperoxia are indicated by † $p < .05$ .

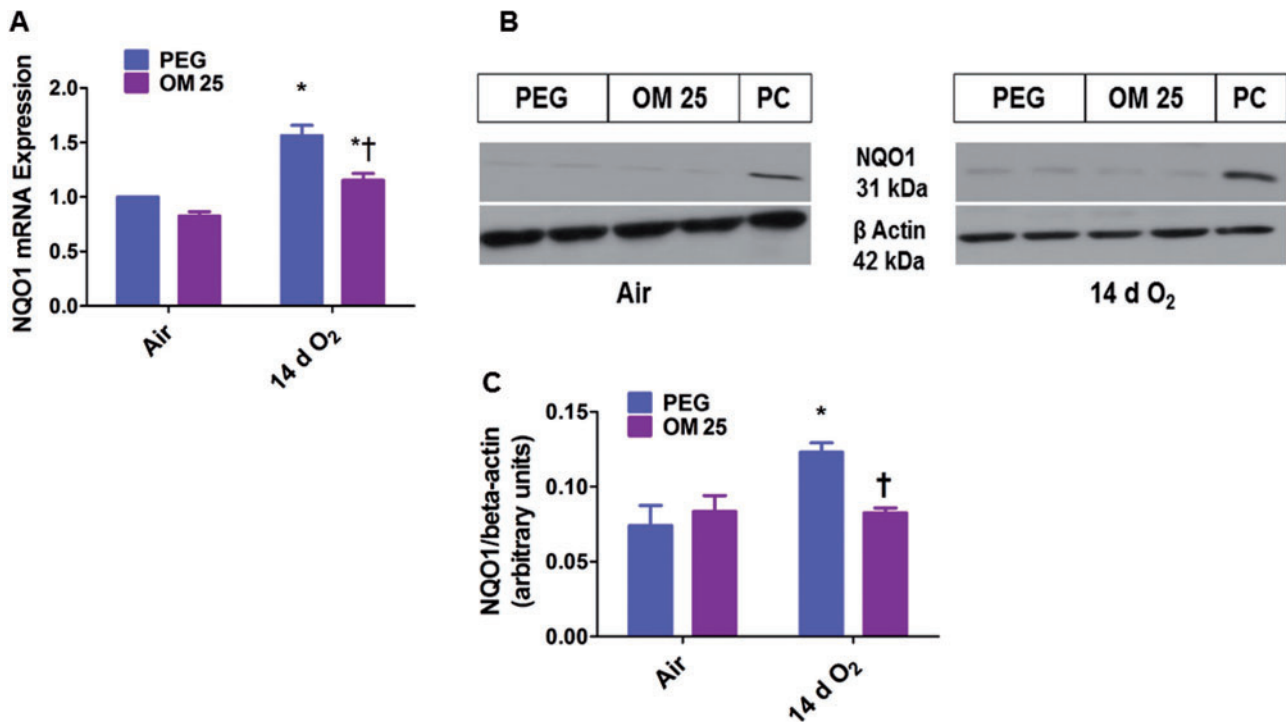


FIG. 8. Two weeks of OM25 therapy in newborn mice decreases hyperoxia-induced pulmonary NQO1 mRNA and protein expression. Newborn mice were treated with PEG or OM25 and exposed to air or hyperoxia for 14 days, following which lung NQO1 mRNA (A) and protein (B) expression were determined by real-time RT-PCR analysis and western blotting, respectively. NQO1 band intensities were quantified and normalized to  $\beta$ -actin (C). Values are means  $\pm$  SEM from at least 6 individual animals per group. Two-way ANOVA showed an effect of hyperoxia and OM25 treatment and an interaction between them for the dependent variable, NQO1. Significant differences between air-breathing and hyperoxia-exposed animals are indicated by \* $p < .05$ . Significant differences between vehicle and OM-treated mice exposed to hyperoxia are indicated by † $p < .05$ .



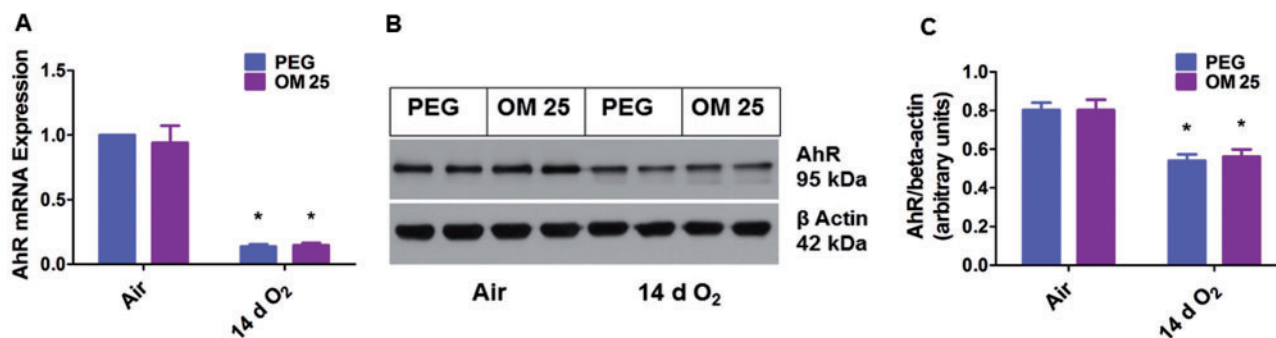


FIG. 9. Two weeks of OM25 therapy in newborn mice does not affect pulmonary AhR mRNA and protein expression. Newborn mice were treated with PEG or OM25 and exposed to air or hyperoxia for 14 days, following which pulmonary AhR mRNA (A) and protein (B) expression were determined by real-time RT-PCR analysis and western blotting, respectively. AhR band intensities were quantified and normalized to  $\beta$ -actin (C). Values are means  $\pm$  SEM from at least 6 individual animals per group. Two-way ANOVA showed an effect of only hyperoxia and not of OM25 treatment on the dependent variable, AhR. Significant differences between air breathing and hyperoxia-exposed animals are indicated by \* $p < .05$ .

alveolar and pulmonary vascular simplification in OM25-treated mice (Figs. 2F, 2G, 2H and 3F, 3G) indicates that OM25 potentiates HDLI in newborn mice. Since we did not observe any significant differences between PEG or OM10-treated mice on hyperoxia-induced alveolar and pulmonary vascular simplification (Figs. 2 and 3) and lung macrophage influx (Fig. 5), we collected lung tissues from PEG or OM25-treated mice for our remaining studies. Pulmonary vascular and alveolar development are highly orchestrated interdependent processes and studies clearly support this concept by demonstrating that an interruption of distal lung angiogenesis secondary to decreased expression of VEGF and/or its signaling receptor, VEGFR2, leads to alveolar simplification (McGrath-Morrow *et al.*, 2005; Thebaud and Abman, 2007). Our findings of hyperoxia-induced decrease in VEGFR2 (Figs. 4A–C) and VEGF (Figs. 4D–F) expression are in agreement with other studies (Hosford and Olson, 2003; Thebaud *et al.*, 2005). Although, VEGF levels (Figs. 4D–F) and VEGFR2 mRNA (Fig. 4A) expression were similar between vehicle and OM25-treated mice exposed to hyperoxia, the augmented decrease in VEGFR2 protein levels in the latter group (Fig. 4B and 4C) indicates that OM25 interrupts lung development partly due to a decrease in VEGFR2 by unknown posttranscriptional mechanisms.

Inflammation plays a key role in the pathogenesis of BPD in preterm infants (Saugstad, 2003). Lung macrophage infiltration is an important marker of a chronic inflammatory state that is associated with BPD (Clement *et al.*, 1988). Our findings (Fig. 5) are consistent with other investigators (Rogers *et al.*, 2011) who have suggested that lung macrophage influx may be an important mediator of hyperoxia-induced lung injury in mice. In addition to inflammation, hyperoxia-induced ROS generation contributes to chronic pulmonary toxicity such as BPD by altering signal transduction pathways and modifying the structure and function of protein, lipids, and DNA (Bhandari, 2010; Saugstad, 2010). However, it is difficult to measure and characterize ROS in real time as they are very unstable. Hence, we determined the expression of MDA-protein adducts and NT, which are stable aldehyde end products of ROS-mediated lipid peroxidation (Moore and Roberts, 1998) and superoxide/peroxynitrite-mediated protein nitration (Ischiropoulos, 1998), respectively. In addition, they are well recognized markers of oxidative stress and tissue damage (Del Rio *et al.*, 2005). Our finding of hyperoxia-induced MDA adducts and NT expression in mice (Fig. 6) are consistent with previous studies (Li *et al.*, 2013; Masood *et al.*, 2010; McGrath-Morrow *et al.*, 2005).

Hyperoxia is known to increase BALF protein levels, which is a marker of increased pulmonary vascular permeability secondary to vascular injury (Britt *et al.*, 2013). However, the increased inflammatory and vascular permeability (Fig. 5) and pro-oxidant (Fig. 6) effects of hyperoxia seen in OM25-treated mice supports the concept that OM25 mediates its effects in part by increasing inflammation, vascular injury, and oxidative stress.

In adult mice, we demonstrated that OM attenuates HLI and inflammation via AhR-dependent mechanisms (Shivanna *et al.*, 2011b). Additionally, OM has a direct scavenging activity against oxygen free radicals and inhibits neutrophil function (Wandall, 1992; Yoshida *et al.*, 2000), and protects against necrotizing enterocolitis in newborn rats (Cadir *et al.*, 2008). These data suggest that OM has antioxidant and anti-inflammatory properties. However, our results were in contrast to these studies and disprove our hypothesis that OM would protect newborn mice against HDLI. The most plausible reasons for these contrasting results may be related to increased duration of therapy and immaturity of the mouse pups. Some of the other contributory factors may be due to differences in the animal species, organs studied, and the nature and duration of the insult. Although the expression levels of CYP1A enzymes are low at birth and reach adult levels in weeks or months (Johnson *et al.*, 2002; Sonnier and Cresteil, 1998), these enzymes can be modulated by AhR agonists or antagonists in the embryonic and neonatal period resulting in various developmental defects (Furness and Whelan, 2009). To address our unexpected results, we determined the effects of prolonged (2 weeks) OM therapy on pulmonary AhR activation since our dose response studies were limited to 4 days in air-breathing mice. Surprisingly, OM therapy for 2 wks attenuated transcriptional activation of the AhR-regulated CYP1A1 enzyme both in air and hyperoxic conditions (Fig. 7). So, we investigated the expression of pulmonary AhR in our experimental model. Our results suggest that prolonged OM25 therapy does not affect the pulmonary AhR expression (Fig. 9) indicating that the decreased CYP1A1 expression is probably secondary to attenuated AhR activation rather than due to decreased AhR levels. The discrepancy between CYP1A1 mRNA and protein levels in hyperoxic conditions may be related to factors such as posttranscriptional modification or protein stabilization. Hyperoxia-induced increase in NQO1 expression despite the low AhR levels in our model (Fig. 8) suggests that this enzyme might be regulated by other transcription factors such as Nrf2. However, attenuation of this effect in OM25-treated animals that have decreased AhR activation (Fig. 8) suggests that

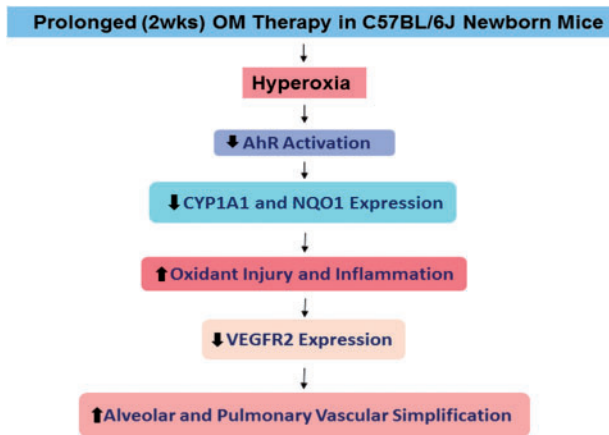


FIG. 10. Proposed mechanism(s) by which OM25 potentiates HDLI in newborn mice: Prolonged (2 weeks) OM25 therapy in newborn mice potentiates HDLI by mechanisms associated with decreased AhR signaling and VEGFR2 expression. AhR, aryl hydrocarbon receptor; CYP1A1, cytochrome P450 1A1; NQO1, NAD(P)H quinone oxidoreductase 1; VEGFR2, vascular endothelial growth factor receptor 2.

AhR partly contributes to the increase in NQO1 expression under hyperoxic conditions. Although the molecular mechanisms of these observations is beyond the scope of this study, it might be due to factors such as increased ROS generation that may competitively inhibit the transcription of these genes at the promoter level and altered miRNA profile that can inhibit the translation of these genes. The protective effects of CYP1A enzymes against HLI in rodents have been extensively documented (Couroucli *et al.*, 2011; Jiang *et al.*, 2004; Mansour *et al.*, 1988; Moorthy, 2008). In addition, NQO1 has been shown to protect cells and tissues against oxidant injury induced by various toxic chemicals (O'Brien, 1991) and oxygen (Das *et al.*, 2006). The protective mechanisms of these enzymes have been attributed to their ability to conjugate and scavenge the reactive electrophiles and lipid peroxidation products generated by an oxidant injury (Cho *et al.*, 2002). Thus, OM25-mediated oxidative stress and hyperoxic injury may be attributed to the deficiency of these AhR-regulated enzymes.

In summary, we demonstrate that prolonged (2 weeks) OM25 therapy decreases pulmonary AhR activation and potentiates hyperoxia induced: (1) alveolar and pulmonary vascular simplification; (2) inflammation; (3) vascular injury; and (4) oxidative stress. We propose that prolonged OM therapy in newborn mice increases HDLI via mechanisms entailing decreased AhR activation that leads to attenuated AOE expression, thereby increasing hyperoxia-induced lung inflammation and oxidative stress, which is known to decrease VEGFR2 expression, the end result of all of which is increased alveolar and pulmonary vascular simplification (Fig. 10). Our findings remains consistent with the conclusion that a functional AhR response is protective in hyperoxia and thus AhR may be a potential therapeutic target to improve current therapies of BPD in preterm infants.

## FUNDING

National Institutes of Health (K08 HD073323 to B.S. and R01 ES009132, R01 HL112516, R01 HL087174, and R01 ES019689 to B.M.); and American Heart Association (BGIA 20190008 to B.S). The study sponsors had no involvement in study design, data collection, analysis and interpretation, writing

of the report or decision to submit the article for publication.

## ACKNOWLEDGMENTS

We thank Pamela Parsons for her timely processing of histopathology and immunohistochemistry slides and Dr Roberto Barrios for his help in evaluating the histology and immunohistochemistry slides.

## REFERENCES

- Abbott, B. D., Birnbaum, L. S., and Perdeu, G. H. (1995). Developmental expression of two members of a new class of transcription factors: I. Expression of aryl hydrocarbon receptor in the C57BL/6N mouse embryo. *Dev. Dyn.* **204**, 133–143.
- Baglole, C. J., Maggirwar, S. B., Gasiewicz, T. A., Thatcher, T. H., Phipps, R. P., and Sime, P. J. (2008). The aryl hydrocarbon receptor attenuates tobacco smoke-induced cyclooxygenase-2 and prostaglandin production in lung fibroblasts through regulation of the NF-kappaB family member RelB. *J. Biol. Chem.* **283**, 28944–28957.
- Bhandari, V. (2010). Hyperoxia-derived lung damage in preterm infants. *Semin. Fetal Neonatal. Med.* **15**, 223–229.
- Bradford, M. M. (1976). A rapid and sensitive method for the quantitation of microgram quantities of protein utilizing the principle of protein-dye binding. *Anal. Biochem.* **72**, 248–254.
- Britt, R. D., Jr, Velten, M., Tipple, T. E., Nelin, L. D., and Rogers, L. K. (2013). Cyclooxygenase-2 in newborn hyperoxic lung injury. *Free Radic. Biol. Med.* **61**, 502–511.
- Cadir, F. O., Bicakci, U., Tander, B., Kilicoglu-Aydin, B., Rizalar, R., Ariturk, E., Aydin, O., and Bernay, F. (2008). Protective effects of vitamin E and omeprazole on the hypoxia/reoxygenation induced intestinal injury in newborn rats. *Pediatr. Surg. Int.* **24**, 809–813.
- Carver, L. A., and Bradfield, C. A. (1997). Ligand-dependent interaction of the aryl hydrocarbon receptor with a novel immunophilin homolog in vivo. *J. Biol. Chem.* **272**, 11452–11456.
- Cho, H. Y., Jedlicka, A. E., Reddy, S. P., Kensler, T. W., Yamamoto, M., Zhang, L. Y., and Kleeberger, S. R. (2002). Role of NRF2 in protection against hyperoxic lung injury in mice. *Am. J. Respir. Cell Mol. Biol.* **26**, 175–182.
- Clement, A., Chadelat, K., Sardet, A., Grimfeld, A., and Tournier, G. (1988). Alveolar macrophage status in bronchopulmonary dysplasia. *Pediatr. Res.* **23**, 470–473.
- Cooney, T. P., and Thurlbeck, W. M. (1982). The radial alveolar count method of Emery and Mithal: a reappraisal 1–postnatal lung growth. *Thorax* **37**, 572–579.
- Couroucli, X. I., Liang, Y. H., Jiang, W., Wang, L., Barrios, R., Yang, P., and Moorthy, B. (2011). Prenatal administration of the cytochrome P4501A inducer, Beta-naphthoflavone (BNF), attenuates hyperoxic lung injury in newborn mice: implications for bronchopulmonary dysplasia (BPD) in premature infants. *Toxicol. Appl. Pharmacol.* **256**, 83–94.
- Das, A., Kole, L., Wang, L., Barrios, R., Moorthy, B., and Jaiswal, A. K. (2006). BALT development and augmentation of hyperoxic lung injury in mice deficient in NQO1 and NQO2. *Free Radic. Biol. Med.* **40**, 1843–1856.
- Del Rio, D., Stewart, A. J., and Pellegrini, N. (2005). A review of recent studies on malondialdehyde as toxic molecule and biological marker of oxidative stress. *Nutr. Metab. Cardiovas. Dis.* **15**, 316–328.

- Denis, M., Cuthill, S., Wikstrom, A. C., Poellinger, L., and Gustafsson, J. A. (1988). Association of the dioxin receptor with the Mr 90,000 heat shock protein: a structural kinship with the glucocorticoid receptor. *Biochem. Biophys. Res. Commun.* **155**, 801–807.
- Diaz, D., Fabre, I., Daujat, M., Saint Aubert, B., Bories, P., Michel, H., and Maurel, P. (1990). Omeprazole is an aryl hydrocarbon-like inducer of human hepatic cytochrome P450. *Gastroenterology* **99**, 737–747.
- Fanaroff, A. A., Stoll, B. J., Wright, L. L., Carlo, W. A., Ehrenkranz, R. A., Stark, A. R., Bauer, C. R., Donovan, E. F., Korones, S. B., Laptook, A. R., et al. (2007). Trends in neonatal morbidity and mortality for very low birthweight infants. *Am. J. Obstet. Gynecol.* **196**, 147 e141–148.
- Favreau, L. V., and Pickett, C. B. (1991). Transcriptional regulation of the rat NAD(P)H:quinone reductase gene. Identification of regulatory elements controlling basal level expression and inducible expression by planar aromatic compounds and phenolic antioxidants. *J. Biol. Chem.* **266**, 4556–4561.
- Fujisawa-Sehara, A., Sogawa, K., Yamane, M., and Fujii-Kuriyama, Y. (1987). Characterization of xenobiotic responsive elements upstream from the drug-metabolizing cytochrome P-450c gene: a similarity to glucocorticoid regulatory elements. *Nucleic Acids Res.* **15**, 4179–4191.
- Furness, S. G., and Whelan, F. (2009). The pleiotropy of dioxin toxicity—xenobiotic misappropriation of the aryl hydrocarbon receptor's alternative physiological roles. *Pharmacol. Ther.* **124**, 336–353.
- Hosford, G. E., and Olson, D. M. (2003). Effects of hyperoxia on VEGF, its receptors, and HIF-2 $\alpha$  in the newborn rat lung. *Am. J. Physiol. Lung Cell. Mol. Physiol.* **285**, L161–L168.
- Husain, A. N., Siddiqui, N. H., and Stocker, J. T. (1998). Pathology of arrested acinar development in postsurfactant bronchopulmonary dysplasia. *Hum. Pathol.* **29**, 710–717.
- Ischiropoulos, H. (1998). Biological tyrosine nitration: a pathophysiological function of nitric oxide and reactive oxygen species. *Arch. Biochem. Biophys.* **356**, 1–11.
- Jiang, W., Welty, S. E., Couroucli, X. I., Barrios, R., Kondraganti, S. R., Muthiah, K., Yu, L., Avery, S. E., and Moorthy, B. (2004). Disruption of the Ah receptor gene alters the susceptibility of mice to oxygen-mediated regulation of pulmonary and hepatic cytochromes P4501A expression and exacerbates hyperoxic lung injury. *J. Pharmacol. Exp. Ther.* **310**, 512–519.
- Jobe, A. J. (1999). The new BPD: an arrest of lung development. *Pediatr. Res.* **46**, 641–643.
- Johnson, T. N., Tanner, M. S., and Tucker, G. T. (2002). Developmental changes in the expression of enterocytic and hepatic cytochromes P4501A in rat. *Xenobiotica* **32**, 595–604.
- Kashfi, K., McDougall, C. J., and Dannenberg, A. J. (1995). Comparative effects of omeprazole on xenobiotic metabolizing enzymes in the rat and human. *Clin. Pharmacol. Therap.* **58**, 625–630.
- Larsson, H., Carlsson, E., Junggren, U., Olbe, L., Sjostrand, S. E., Skanberg, I., and Sundell, G. (1983). Inhibition of gastric acid secretion by omeprazole in the dog and rat. *Gastroenterology* **85**, 900–907.
- Larsson, H., Carlsson, E., Ryberg, B., Fryklund, J., and Wallmark, B. (1988). Rat parietal cell function after prolonged inhibition of gastric acid secretion. *Am J Physiol.* **254**, G33–G39.
- Li, H. D., Zhang, Z. R., Zhang, Q. X., Qin, Z. C., He, D. M., and Chen, J. S. (2013). Treatment with exogenous hydrogen sulfide attenuates hyperoxia-induced acute lung injury in mice. *Eur. J. Appl. Physiol.* **113**, 1555–1563.
- Li, X. Q., Andersson, T. B., Ahlstrom, M., and Weidolf, L. (2004). Comparison of inhibitory effects of the proton pump-inhibiting drugs omeprazole, esomeprazole, lansoprazole, pantoprazole, and rabeprazole on human cytochrome P450 activities. *Drug Metab. Dispos.* **32**, 821–827.
- Lind, T., Cederberg, C., Ekenved, G., Haglund, U., and Olbe, L. (1983). Effect of omeprazole—a gastric proton pump inhibitor—on pentagastrin stimulated acid secretion in man. *Gut* **24**, 270–276.
- Mansour, H., Levacher, M., Azoulay-Dupuis, E., Moreau, J., Marquetty, C., and Gougerot-Pocidallo, M. A. (1988). Genetic differences in response to pulmonary cytochrome P-450 inducers and oxygen toxicity. *J. Appl. Physiol.* **64**, 1376–1381.
- Masood, A., Belcastro, R., Li, J., Kantores, C., Jankov, R. P., and Tanswell, A. K. (2010). A peroxynitrite decomposition catalyst prevents 60% O<sub>2</sub>-mediated rat chronic neonatal lung injury. *Free Radic. Biol. Med.* **49**, 1182–1191.
- McGrath-Morrow, S. A., Cho, C., Cho, C., Zhen, L., Hicklin, D. J., and Tuder, R. M. (2005). Vascular endothelial growth factor receptor 2 blockade disrupts postnatal lung development. *Am J. Resp. Cell Mol. Biol.* **32**, 420–427.
- Moore, K., and Roberts, L. J., 2nd (1998). Measurement of lipid peroxidation. *Free Radic. Res.* **28**, 659–671.
- Moorthy, B. (2008). Cytochromes P450. In *Role in Drug Metabolism and Toxicity of Drugs and Other Xenobiotics*, (C. Ioannides, Ed.), pp. 97–135. RSC Publishing, Cambridge.
- O'Brien, P. J. (1991). Molecular mechanisms of quinone cytotoxicity. *Chem. Biol. Interact.* **80**, 1–41.
- Park, M. S., Rieger-Fackeldey, E., Schanbacher, B. L., Cook, A. C., Bauer, J. A., Rogers, L. K., Hansen, T. N., Welty, S. E., and Smith, C. V. (2007). Altered expressions of fibroblast growth factor receptors and alveolarization in neonatal mice exposed to 85% oxygen. *Pediatr. Res.* **62**, 652–657.
- Pollenz, R. S., Sattler, C. A., and Poland, A. (1994). The aryl hydrocarbon receptor and aryl hydrocarbon receptor nuclear translocator protein show distinct subcellular localizations in Hepa 1c1c7 cells by immunofluorescence microscopy. *Mol. Pharmacol.* **45**, 428–438.
- Rogers, L. K., Valentine, C. J., Pennell, M., Velten, M., Britt, R. D., Dingess, K., Zhao, X., Welty, S. E., and Tipple, T. E. (2011). Maternal docosahexaenoic acid supplementation decreases lung inflammation in hyperoxia-exposed newborn mice. *J. Nutr.* **141**, 214–222.
- Saugstad, O. D. (2003). Bronchopulmonary dysplasia-oxidative stress and antioxidants. *Semin. Neonatol.* **8**, 39–49.
- Saugstad, O. D. (2010). Oxygen and oxidative stress in bronchopulmonary dysplasia. *J. Perinat. Med.* **38**, 571–577.
- Shivanna, B., Chu, C., Welty, S. E., Jiang, W., Wang, L., Couroucli, X. I., and Moorthy, B. (2011a). Omeprazole attenuates hyperoxic injury in H441 cells via the aryl hydrocarbon receptor. *Free Radic. Biol. Med.* **51**, 1910–1917.
- Shivanna, B., Jiang, W., Wang, L., Couroucli, X. I., and Moorthy, B. (2011b). Omeprazole attenuates hyperoxic lung injury in mice via aryl hydrocarbon receptor activation and is associated with increased expression of cytochrome P4501A enzymes. *J. Pharmacol. Exp. Ther.* **339**, 106–114.
- Shivanna, B., Zhang, W., Jiang, W., Welty, S. E., Couroucli, X. I., Wang, L., and Moorthy, B. (2013). Functional deficiency of aryl hydrocarbon receptor augments oxygen toxicity-induced alveolar simplification in newborn mice. *Toxicol. Appl. Pharmacol.* **267**, 209–217.
- Short, E. J., Klein, N. K., Lewis, B. A., Fulton, S., Eisengart, S., Kercksmar, C., Baley, J., and Singer, L. T. (2003). Cognitive and academic consequences of bronchopulmonary dysplasia and very low birth weight: 8-year-old outcomes. *Pediatrics* **112**, e359.

- Sogawa, K., and Fujii-Kuriyama, Y. (1997). Ah receptor, a novel ligand-activated transcription factor. *J. Biochem.* **122**, 1075–1079.
- Sonnier, M., and Cresteil, T. (1998). Delayed ontogenesis of CYP1A2 in the human liver. *Eur. J. Biochem.* **251**, 893–898.
- Tallman, M. N., Ali, S. Y., and Smith, P. C. (2004). Altered pharmacokinetics of omeprazole in cystic fibrosis knockout mice relative to wild-type mice. *Drug Metab. Dispos.* **32**, 902–905.
- Thatcher, T. H., Maggirwar, S. B., Baglole, C. J., Lakatos, H. F., Gasiewicz, T. A., Phipps, R. P., and Sime, P. J. (2007). Aryl hydrocarbon receptor-deficient mice develop heightened inflammatory responses to cigarette smoke and endotoxin associated with rapid loss of the nuclear factor-kappaB component RelB. *Am. J. Pathol.* **170**, 855–864.
- Thebaud, B., Ladha, F., Michelakis, E. D., Sawicka, M., Thurston, G., Eaton, F., Hashimoto, K., Harry, G., Haromy, A., Korbitt, G., et al. (2005). Vascular endothelial growth factor gene therapy increases survival, promotes lung angiogenesis, and prevents alveolar damage in hyperoxia-induced lung injury: evidence that angiogenesis participates in alveolarization. *Circulation.* **112**, 2477–2486.
- Thebaud, B., and Abman, S. H. (2007). Bronchopulmonary dysplasia: where have all the vessels gone? Roles of angiogenic growth factors in chronic lung disease. *Am. J. Respir. Crit. Care Med.* **175**, 978–985.
- Tirona, R. G., and Kim, R. B. (2005). Nuclear receptors and drug disposition gene regulation. *J. Pharm. Sci.* **94**, 1169–1186.
- Tompkins, L. M., and Wallace, A. D. (2007). Mechanisms of cytochrome P450 induction. *J. Biochem. Mol. Toxicol.* **21**, 176–181.
- van Eijl, S., Mortaz, E., Versluis, C., Nijkamp, F. P., Folkerts, G., and Bloksma, N. (2011). A low vitamin A status increases the susceptibility to cigarette smoke-induced lung emphysema in C57BL/6J mice. *J. Physiol. Pharmacol.* **62**, 175–182.
- Wandall, J. H. (1992). Effects of omeprazole on neutrophil chemotaxis, super oxide production, degranulation, and translocation of cytochrome b-245. *Gut.* **33**, 617–621.
- Wei, C., Caccavale, R. J., Weyand, E. H., Chen, S., and Iba, M. M. (2002). Induction of CYP1A1 and CYP1A2 expressions by prototypic and atypical inducers in the human lung. *Cancer Lett.* **178**, 25–36.
- Whitlock, J. P., Jr (1999). Induction of cytochrome P4501A1. *Annu. Rev. Pharmacol. Toxicol.* **39**, 103–125.
- Yoshida, N., Yoshikawa, T., Tanaka, Y., Fujita, N., Kassai, K., Naito, Y., and Kondo, M. (2000). A new mechanism for anti-inflammatory actions of proton pump inhibitors—inhibitory effects on neutrophil-endothelial cell interactions. *Aliment Pharmacol. Ther.* **14** (Suppl. 1), 74–81.
- Zhang, S., Patel, A., Chu, C., Jiang, W., Wang, L., Welty, S. E., Moorthy, B., and Shivanna, B. (2015). Aryl hydrocarbon receptor is necessary to protect fetal human pulmonary microvascular endothelial cells against hyperoxic injury: Mechanistic roles of antioxidant enzymes and RelB. *Toxicol. Appl. Pharmacol.* **286**, 92–101.